HHS Public Access

Author manuscript

Neuroimage. Author manuscript; available in PMC 2017 December 01.

Published in final edited form as:

Neuroimage. 2016 December ; 143: 82–90. doi:10.1016/j.neuroimage.2016.08.040.

Glucose metabolism-weighted imaging with chemical exchange-sensitive MRI of 2-deoxyglucose (2DG) in brain: sensitivity and biological sources

Tao Jin[1,2,*], **Hunter Mehrens**[1], **Ping Wang**[1], and **Seong-Gi Kim**[1,3,4]

[1]NeuroImaging Laboratory, Department of Radiology, University of Pittsburgh, Pittsburgh, PA, 15203

[2]Department of Bioengineering, University of Pittsburgh, Pittsburgh, PA, 15203

[3]Center for Neuroscience Imaging Research, Institute for Basic Science (IBS), Suwon, Korea

[4]Department of Biomedical Engineering, Sungkyunkwan University, Suwon, Korea

Abstract

Recent proof-of-principle studies have demonstrated the feasibility of measuring the uptake and metabolism of non-labelled 2-deoxy-D-glucose (2DG) by a chemical exchange-sensitive spin-lock (CESL) MRI approach. In order to gain better understanding of this new approach, we performed dynamic *in vivo* CESL MRI on healthy rat brains with an intravenous injection of 2DG under various conditions at 9.4 T. For three 2DG doses of 0.25, 0.5 and 1 g/kg, we found that 2DG-CESL signals increased linearly with injection dose at the initial (<20 min) but not the later period (>40 min) suggesting time-dependent differential weightings of 2DG transport and metabolism. Remaining 2DG-CESL studies were performed with 0.25 g/kg 2DG. Since a higher isoflurane level reduces glucose metabolism and increases blood flow, 2DG-CESL was measured under 0.5%, 1.5% and 2.2% isoflurane. The 2DG-CESL signal was reduced at higher isoflurane levels correlating well with the 2DG phosphorylation in the intracellular space. To detect regional heterogeneities of glucose metabolism, 2DG-CESL with 0.33×0.33×1.50 mm^3 resolution was obtained, which indeed showed a higher response in the cortex compared to the corpus callosum. Lastly, unlike CESL MRI with the injection of non-transportable mannitol, the 2DG-CESL response decreased with an increased spin-lock pulse power confirming that 2DG-CESL is dominated by chemical exchange processes in the extravascular space. Taken together, our results showed that 2DG-CESL MRI signals mainly indicate glucose transport and metabolism and may be a useful biomarker for metabolic studies of normal and diseased brains.

[*]Corresponding author: Tao Jin, Ph. D., Department of Radiology, University of Pittsburgh, 3025 E Carson Street, Room 156, Pittsburgh, PA, 15203, (Tel) 412-383-8010. (Fax) 412-383-6799. taj6@pitt.edu.

Keywords

CMRglu; glucose transport; glucose metabolism; PET; MRI; CEST; CESL

Introduction

Glucose uptake and metabolism are sensitive biomarkers for cellular function and many diseases. In particular, the brain relies on glucose for its energy supply, thus the uptake and metabolism of glucose in brain are of particular importance and have often been studied by a glucose analog, 2-deoxy-D-glucose (2DG), in its natural or isotope-labeled forms. In the healthy brain, 2DG is transported across the blood brain barrier (BBB) mainly by glucose transporters to the extracellular space, and then quickly uptake into the cells (Fig. 1A). In most cells, glucose hexokinase phosphorylates 2DG into 2-deoxy-D-glucose-6-phosphate (2DG6P) which cannot be metabolized further and is trapped in the intracellular compartment for many hours (Huang and Veech, 1985; Jain et al., 1985; Sokoloff et al., 1977). Thus, labeled forms of 2DG, such as by radioisotope carbon-14 or fluorine-18, serve as good markers for tissue glucose uptake and hexokinase activity and have been widely applied in autoradiography (Huang and Veech, 1985; Sokoloff et al., 1977) or PET (Fox and Raichel, 1984; Ido et al., 1978). The autoradiography method has high spatial resolution but is exclusively limited to animal studies and can only be obtained at a single time point due to the requirement of histology. The PET technique has poor spatial resolution due to the size of PET detectors and intrinsic fluorine-18-induced positron signal blurring of 0.54 mm full-width at half maximum (Moses, 2011), and the radiation exposure limits the scan frequency and excludes certain patient groups (de Leon et al., 2001; Heiss et al., 1993; Ma and Eidelberg, 2007; Matz et al., 2006; Silverman et al., 2001; Yong et al., 2007).

Similar to the PET approach, ^{13}C-labeled 2DG can be injected and the dynamics can be detected by ^{13}C NMR spectroscopy. After initial successful studies with a pharmological dose (e.g., 0.5 g/kg) (Cohen et al., 2002; Kotyk et al., 1989), this NMR method has not been widely utilized due to the requirement of expensive ^{13}C-labeled 2DG, and the sensitivity is too low to be applied for imaging studies. The detectibility of 2DG can be enhanced by the emerging chemical exchange-sensitive saturation transfer (CEST) or spin lock (CESL) MRI techniques (Chan et al., 2012; Jin et al., 2014; Nasrallah et al., 2013; Rivlin et al., 2013; Walker-Samuel et al., 2013; Zu et al., 2014), in which non-labeled D-glucose or 2DG can be indirectly detected from a reduction of the water signal induced by the fast chemical exchange between hydroxyl (i.e., -OH group in Fig. 1A) and water protons. These techniques are referred to as glucoCEST or glucoCESL and they detect signal changes in tissue caused by an administration of glucose or glucose analogs. The difference between them is which spins (hydroxyl vs. water protons) are irradiated during the chemical exchange-sensitizing period. CESL MRI with glucose analog 2DG is hereafter referred to as 2DG-CESL for emphasizing the injection of 2DG, which is used interchangeably with glucoCESL. Compared to direct measurement of glucose with proton NMR spectroscopic methods, indirect measurement with glucoCEST or glucoCESL offers a sensitivity enhancement of about 2 orders of magnitude.

The sensitivity of CEST or CESL is still much lower than FDG-PET or autoradiography. In proof-of-principle MRI studies, a high 2DG dose of at least 0.5 g/kg has been adopted in studies of normal animal brains (Jin et al., 2014; Nasrallah et al., 2013; Zu et al., 2014) and 1–2 g/kg in tumor-bearing mice (Rivlin et al., 2013). Such a high dose can competitively inhibit D-glucose utilization leading to intracellular glucopenia in the central nervous system and severely affecting the systemic physiology. Thus, it is critically important to reduce 2DG dosage even in preclinical studies. Secondly, because the injected 2DG is indirectly detected through a change of water signals, the signal source of glucoCEST or glucoCESL is complex and not fully understood. For example, it is controversial whether the glucoCEST signal with D-glucose injection in tumors contains both intracellular and extracellular components (Walker-Samuel et al., 2013) or is mainly due to the transport and leakage of D-glucose to the extracellular space (Chan et al., 2012). Additionally, these signals may have contributions from non-glucose related components such as shifts in water due to osmolality differences.

In our initial signal source study (Jin et al., 2014), we found that glucoCESL signal has negligible contributions from intravascular blood at 9.4 T and a small contribution from the osmolality effect induced by the intravenous injection of hypertonic solution. In this study, sensitivity and biological sources of CESL, after the administration of 2DG, were systematically examined in healthy isoflurane-anesthetized rats at 9.4 T for mapping glucose metabolic indices (Fig. 1B). Since glucoCESL likely has a higher sensitivity than glucoCEST (Jin et al., 2014; Zu et al., 2014), glucoCESL was used in our studies. 1) Three different 2DG doses (0.25, 0.5 and 1 g/kg) were used to determine the sensitivity limit under our settings and the dose-dependent temporal characteristics of 2DG-CESL signals. 2) Since a higher isoflurane level decreases cerebral metabolic rate of glucose (CMRglu) but increases cerebral blood flow (CBF) (Maekawa et al., 1986), isoflurane level was varied from 0.5% to 2.2% to determine whether 2DG-CESL is correlated with metabolism or blood flow. 3) High-spatial resolution studies were performed to compare CESL response at various brain regions. 4) To characterize the source of 2DG-CESL, spin lock power-dependent $R_1\rho$ changes were compared to those obtained with mannitol, which is not transportable to the extravascular space but can induce similar osmolality changes as 2DG..

Materials and methods

GlucoCESL MRI approach: implementation and theory

The pulse sequence for the glucoCESL MRI technique has two components (Fig. 1C); the first module is for on-resonance (i.e., water) spin-lock preparation, and the second module is for image acquisition. In the 1st module, an adiabatic spin-lock preparation was adopted because it is less susceptible to B_0 and B_1 inhomogeneities. Briefly, a 2-ms adiabatic half passage (AHP) pulse was followed by a ramp of 0.5 ms during which the amplitude of the on-resonance RF pulse was decreased to the desired spin-lock power and then held constant for the spin-locking time (TSL) (Grohn et al., 2005; Jin and Kim, 2010). This was then followed by an inverted AHP pulse (Garwood and DelaBarre, 2001) which returns the magnetization to the Z-axis for imaging. After the spin-lock preparation and the crush of residual magnetization in the X–Y plane, MR images can be acquired by fast imaging

techniques such as a spin-echo echo planar imaging (EPI) technique. At given TSL and TE values, the signal can be expressed as

$$S=S_0 \cdot \exp(-TSL \cdot R_{1\rho}) \cdot \exp(-TE \cdot R_2) \quad [1]$$

where S_0 is the signal intensity when TSL and TE values equal 0. A time series of $T_1\rho$ (=1/$R_1\rho$) weighted images with varied TSL (and same TE) were acquired with a bolus injection of glucose or analogs (Fig. 1D). Then a time series of $R_1\rho$ maps was calculated by pixel-wise fitting of the TSL-dependent signals to Eq. [1].

Assuming a two-pool exchange process where the relative population of labile to water protons, p, is much smaller than 1, $R_1\rho$ can be expressed as (Jin et al., 2011; Trott and Palmer, 2002)

$$R_{1\rho}=\frac{p \cdot k \cdot \delta^2}{\delta^2+\gamma^2 B_1^2+k^2}+R_{2,0}, \quad [2]$$

where γ is the gyromagnetic ratio, k and δ is the exchange rate and chemical shift between protons in water and labile protons (e.g., the hydroxyl groups of 2DG or 2DG6P), respectively, and $R_{2,0}$ is the transverse relaxation rate of water protons without chemical exchange contributions. $\Delta R_1\rho$ after the administration of 2DG can be expressed as

$$\Delta R_{1\rho}=\frac{\Delta p \cdot k \cdot \delta^2}{\delta^2+\gamma^2 B_1^2+k^2}+\Delta R_{2,0}, \quad [3]$$

where the 1st term indicates the contribution from the increase of the total hydroxyl concentration, and $\Delta R_{2,0}$ indicates the contribution from all non-chemical-exchange related effects. $\Delta R_{2,0}$ can be caused by a change of relative volume fractions in compartments with different $R_{2,0}$ values (e.g., blood vs. tissue, or cerebrospinal fluid vs. tissue). For example, a shift of water between blood and extravascular tissue may occur due to the intravenous injection of hypertonic solution. Eq. [3] indicates that a higher γB_1 can reduce the exchange-mediated term (the first term) but not the non-chemical exchange-related $\Delta R_{2,0}$ term. To separate these two terms, the spin-lock power (γB_1) can be modulated; the B_1-dependent component of $\Delta R_1\rho$ is related to a change in the exchange-mediated relaxation caused by the injected glucose analogs, while the B_1-independent component is related to non-chemical exchange effects.

Animal preparation

A total of 46 male Sprague-Dawley rats weighing 225 to 366 g were studied with the approval by the Institutional Animal Care and Use Committee at the University of Pittsburgh. Initially, the animals were anesthetized with isoflurane (5% for induction and 2% during surgery) in a mixture of O_2 and air gases with the O_2 concentration kept at 30% throughout the experiment. The right femoral vein was catheterized for the injection of

glucose analogs and for the delivery of maintenance fluid with pancuronium bromide to suppress animal motions (0.2 mg/kg initial bolus followed by infusion with a rate of 0.2 mg/kg/hour) when a low isoflurane level was used. The right femoral artery was catheterized to monitor the arterial blood pressure. For MR experiments, the isoflurane level was adjusted to 1.5 % with the use of a nose cone or 0.5% and 2.2% with intubation. The blood pressure and end-tidal CO_2 were maintained at a normal physiological condition. The rectal temperature was maintained at 37.0 ± 0.5°C using a feedback-controlled heating pad.

In vivo MRI experiments

All experiments were performed on a 9.4 T magnet equipped with an actively shielded 12-cm gradient system (Magnex, UK), interfaced to a DirectDrive 2 console (Agilent, Santa Clara, CA, USA). A detunable volume excitation (6.4-cm diameter) and surface receiver coil combination (2.2-cm diameter) (Nova Medical Inc, Massachusetts, USA) were used for low-resolution studies (Fig. 1B), and a 3.8-cm ID birdcage volume coil (Virtumed LLC, Minneapolis, Minnesota) was used for high-resolution studies. In all experiments, B_1 maps were first obtained (Jin and Kim, 2010). Since the change in $R_1\rho$ induced by administered glucose analogs is relatively small, it is critical to maintain stable animal conditions during glucoCESL experiments. Thus, we performed glucoCESL experiments after waiting at least 0.5 to 1 hour for the animal condition (e.g., body temperature and anesthesia) to be stabilized inside the magnet.

Spin-lock MRI images were continuously acquired during a 30 – 60 min pre-injection and 80 – 120 min post-injection period (see Fig. 1D). Imaging parameters were field of view = 32 mm × 32 mm, 2 or 3 slices, and repetition time (TR) = 3 s. Images with (i) TSL = 0 and (ii) TSL = 50 ms and γB_1 = 500 Hz were interleaved for Paradigms 1, 2, and 3, and images with (i) TSL = 0, (ii) TSL = 50 ms and γB_1 = 300 Hz, and (iii) TSL = 50 ms and γB_1 = 3000 Hz were interleaved for Paradigm 4. When TSL was 0, a delay time following each data acquisition was increased by 50 ms to maintain constant repetition time. 2DG and mannitol solutions were prepared at 25% weight by volume in saline (e.g., 0.25 g/ml), and each dose was injected to the femoral vein over a 1 – 2 min period. Only one injection was performed for each animal. In experiments with 2 g/kg of 2DG (n = 3), all animals died within 30 minutes after injection. Additionally, seven sets of animal data were excluded due to excessive animal motion (i.e., imperfect fixation of animal heads) or accidental death during the experiment. Datasets for the four paradigms were obtained from the remaining thirty-six animals.

Paradigm 1 2DG-dose dependency: A dose of 0.25 g/kg (n = 5 rats), 0.5 g/kg (n = 6), and 1 g/kg (n = 3) of 2DG was injected to determine dose-dependent 2DG-CESL signals under 1.5% isoflurane. Single-shot spin-echo EPI images with a matrix size of 64 × 64, and a slice thickness of 2 mm and TE of 30 ms were acquired for TSL = 0 and TSL = 50 ms with γB_1 = 500 Hz. Since baseline signal intensities of brain in the images with TSL= 50 ms were only ~1/3 of those with TSL = 0 ms, images with TSL of 50 ms were acquired 3 times more to enhance the sensitivity. One repeating unit was TSL = 0, 50, 50, and 50 ms, yielding a temporal resolution of 12 s (Fig. 1D). The 1 g/kg 2DG data were combined with a previous

study (n = 4) with the same setting and identical parameters (Jin et al., 2014), yielding a total of n = 7 for the 1 g/kg dose.

Paradigm 2 Anesthesia level dependency: 2DG-CESL images were obtained with 0.25 g/kg 2DG injection, under isoflurane anesthesia of 0.5% (n = 6) and 2.2% (n = 4). The imaging parameters used were same as Paradigm 1. The results were compared with those of 0.25 g/kg injection under 1.5% isoflurane in Paradigm 1.

Paradigm 3 High-resolution 2DG-CESL imaging: To examine regional heterogeneities of the 2DG-CESL signals, high spatial resolution studies (n = 4) were performed where 0.25 g/kg 2DG was injected under 0.5% isoflurane. Two-shot spin-echo EPI images were obtained with a matrix size of 96 × 96 (zero-filled to 128 × 128), a slice thickness of 1.5 mm, TE of 8.5 ms, and TR for each shot of 3 s. Spin-lock parameters were same as those in Paradigm 1 and 2. Each repeating unit was TSL = 0, 50, 50, and 50 ms, yielding a temporal resolution of 24 s. T_1-weighted spinecho EPI images (inversion time = 1.4 s and TR = 4 s) were also acquired to compare with the 2DG-CESL maps.

Paradigm 4 Sources of 2DG-CESL signals: To study the sources of the 2DG-CESL signals, CESL images were compared for two γB_1 values of 300 Hz and 3000 Hz with 0.25 g/kg 2DG injection under 0.5% isoflurane (n = 4). Imaging parameters were the same as those in Paradigm 3. Each repeating unit consisted of three images: i) TSL of 0 ms, ii) TSL of 50 ms and γB_1 of 300 Hz, and iii) TSL of 50 ms and γB_1 of 3000 Hz, yielding a temporal resolution of 18 s. While 2DG can be quickly transported across the BBB and taken up by cells and phosphorylated into 2DG6P, mannitol induces similar osmolality effects but cannot be transported across the BBB (Thenuwara et al., 2002). Thus, mannitol can be used as an "osmolality control". Since our pilot study showed that the glucoCESL response with mannitol is much smaller than that with 2DG, a higher dose of 1 g/kg (n = 4) was used to enhance sensitivity.

Data analysis

Data were analyzed with in-house Matlab® programs and STIMULATE software (Strupp, 1996). In each repeating unit, consecutively acquired images with TSL of 50 ms were averaged. Time series of images with the same spin-lock parameters were first extracted from each study, and time series of $R_1\rho$ images were calculated by $ln\,(S_{TSL=0} / S_{TSL=50\ ms}) / 50$ ms where $S_{TSL=0}$ and $S_{TSL=50\ ms}$ is the signal intensity of TSL = 0 and 50 ms, respectively. Thus, a time series of $R_1\rho$ with γB_1 = 500 Hz was generated in Paradigms 1, 2, 3, while two time series of $R_1\rho$ with γB_1 = 300 Hz and 3000 Hz were generated in Paradigm 4.

To obtain statistical maps, the Students' *t*-test was performed to compare pre- vs. post-injection images on a pixel-by-pixel basis. Baseline pre-injection images were defined as data spanning 30 minutes before the start of injection while post-injection images were from data spanning 20–60 minutes post-injection except in Paradigm 1. The $R_1\rho$ change or *t*-value maps were obtained where a threshold of $p < 0.05$ and a minimum cluster size of 3 pixels were applied. A threshold of baseline $R_1\rho$ value of 20 s^{-1} was additionally applied to exclude pixels with significant partial volume fractions of cerebrospinal fluid (CSF) (except

Fig. 6) because $\Delta R_1\rho$ can be induced by a change of volume fractions between tissue and CSF which have different $R_1\rho$ values (2.5 s^{-1} for CSF vs. 23 s^{-1} for tissue) (Jin and Kim, 2010).

Quantitative region of interest (ROI) analyses were performed for the cortex and additionally for the corpus callosum and globus pallidus for Paradigm 3. Time courses were obtained by averaging signals from all pixels within ROIs and interpolated to 1-minute intervals. Data are shown as mean ± standard deviation (SD).

Results

Characteristics of spin-echo images vs. chemical exchange-sensitive spin-lock images

To obtain chemical exchange-sensitive contrast, time series of two brain images were acquired: spin-echo EPI images without spin lock and the same spin-echo EPI readout preceded by a spin-lock preparation of 50 ms. With the injection of 0.5 g/kg of 2DG in 1.5% isoflurane anesthetized rats, negative signal changes (blue to purple pixels in Fig. 2A and time courses in Fig. 2B–C) were observed in the spin-echo imaging data with TE of 30 ms and TSL of 0. Since R_2 relaxation is an extreme case of spin-lock with $\gamma B_1 = 0$ (see Eq. [2]), spin-echo images with a relatively long echo time of 30 ms were sensitive to susceptibility changes (such as BOLD effects) in addition to chemical exchange-mediated relaxation which increases after 2DG injection (see black time courses in Fig. 2B–C). In the time series with TSL = 50 ms, additional relaxation due to an increase in chemical exchange-induced $R_1\rho$ caused a much larger signal decrease (Fig. 2A; see red time courses in Fig. 2B–C). When $R_1\rho$ was calculated from the data with TSL = 0 and 50 ms, the R_2-related effect during the same TE was removed. An increase in $R_1\rho$ was detected in most brain regions (Fig. 2A). Especially, $\Delta R_1\rho$ increased slowly, but continuously over 90 min after the 2DG injection. It should be noted that blood 2DG peaked immediately after injection, thus the $\Delta R_1\rho$ induced by 2DG injection originates from the extravascular space (Jin et al., 2014).

2DG dose dependency for determining the dynamic characteristics and detection limit (Paradigm 1)

To examine dose-dependent response, 0.25, 0.5 and 1 g/kg 2DG were used under 1.5% isoflurane and time courses were obtained from cortical ROIs (Fig. 3A). When 1 g/kg 2DG was injected, the $R_1\rho$ change increased rapidly, reached a peak at ~20 min post injection and then slowly decreased. For two lower doses, the $R_1\rho$ increased faster in the initial ~20 min, and slowly during the rest of experimental time. Initial uptake slope was closely related to the injected 2DG dose, suggesting that 2DG transport is dominant at early time points. To evaluate time-dependent magnitude changes, $\Delta R_1\rho$ values of each 30-min period were averaged. The $\Delta R_1\rho$ for the initial 5 to 30 min post injection was almost linearly dependent on the 2DG dose (black points in Fig. 3B). However, the change of $R_1\rho$ at later time points deviated from linear dependency (red and green points in Fig. 3B), likely due to a slower increase of 2DG6P trapped in the intracellular space (Kotyk et al., 1989). Because the accumulation of 2DG6P is limited by the amount of hexokinase and the rate of phosphorylation, it is not linearly proportional to the dosage of 2DG injection. This sub-linear dose dependence agrees with a recent glucoCEST study which reported that after 0.5

g/kg and 1 g/kg of 2DG injection, the increase of 2DG6P concentration is similar (<~20% difference) (Nasrallah et al., 2013). Since the 2DG6P accumulation is slower than 2DG transport, it is plausible that early data points are heavily weighted to extravascular 2DG (both intracellular and extravascular-extracellular) which reflects glucose transport, whereas later $R_1\rho$ changes have more contribution from the intracellular accumulation of 2DG6P which reflects glucose metabolism. For long measurement studies (>30 min), significant 2DG-CESL signal changes were robustly observed for all three 2DG doses. Therefore, we used the lowest 2DG dose of 0.25 g/kg for the remaining experiments to mitigate intracellular glucopenia induced by 2DG injection.

Anesthesia level dependency for examining source of 2DG-CESL (Paradigm 2)

Our data in Paradigm 1 indicate that 2DG-CESL originates from the extravascular space and suggest an increasing contribution from glucose metabolism at later periods after injection. To further investigate whether 2DG-CESL is indeed sensitive to glucose metabolism or is strongly affected by cerebral blood flow, we measured 2DG-CESL with varying isoflurane anesthesia levels, because higher isoflurane levels reduce CMRglu but increases CBF (Maekawa et al., 1986). The CESL signal responses from a 0.25 g/kg 2DG injection were compared for three isoflurane levels of 0.5%, 1.5% and 2.2% (Fig. 4). Clearly, a lower isoflurane level induced a higher $R_1\rho$ increase (Fig. 4). The 2DG-CESL response is significant in cortical areas but did not pass detection thresholds in some subcortical brain regions (green arrows). The magnitude of $\Delta R_1\rho$ was larger for the 0.5% isoflurane level than higher isoflurane levels (Fig. 4B) correlating well with glucose metabolic rates (e.g., 2DG6P accumulation in the intracellular space). At 0.5, 1.5, and 2.2% isoflurane levels, the averaged $\Delta R_1\rho$ from 40 to 60 min after injection was 0.43, 0.30, and 0.17 s^{-1}, and the averaged $\Delta R_1\rho$ from 60 to 90 min was 0.45, 0.33, and 0.19 s^{-1}, respectively.

High-resolution glucoCESL for detecting differences in regional glucose metabolism (Paradigm 3)

The low-resolution study of Fig. 4 suggested that glucoCESL signal has some regional heterogeneities. It is known that the brain glucose metabolism is highly region-dependent, and the CMRglu of cortical gray matter is higher than that of white matter and the globus pallidus (Maekawa et al., 1986). To better determine region-specific glucoCESL responses of 2DG, high-resolution studies with 333×333×1500 μm^3 were performed under 0.5% isoflurane (Fig. 5). The cortical region has higher intensity than the corpus callosum (blue arrows) and the globus pallidus (red arrow). In ROIs determined from the T_1-weighted anatomical images, the $R_1\rho$ change averaged over a 50–75 min post-injection period (Fig. 5B) is ~63% and ~68% higher in the cortex than the corpus callosum and globus pallidus, respectively.

Source of glucoCESL: chemical exchange vs. non-chemical exchange (Paradigm 4)

The three experiments described above suggest that the late response of 2DG-CESL is sensitive to glucose metabolism but not to cerebral blood flow. However, it is still unclear whether this metabolic contribution is dominant or there are other contaminations unrelated to 2DG uptake and metabolism. To examine this issue, the CESL results of 1 g/kg mannitol were compared with those of 0.25 g/kg 2DG at two γB_1 values of 300 Hz and 3000 Hz. The

spatial patterns of the $\Delta R_1\rho$ map are similar for the two injections. In the ventricle area (blue arrows), a large $R_1\rho$ increase can be detected which is similar for both 300 Hz and 3000 Hz, likely due to a decrease in the CSF volume fraction (Jin and Kim, 2010). In the brain areas, the spin-lock power-dependent time courses are quite different. 1) The $\Delta R_1\rho$ with mannitol injection is similar for the two spin-lock powers of 300 Hz vs. 3000 Hz (Fig. 6B). In contrast, with 2DG injection $\Delta R_1\rho$ is highly dependent on γB_1 (Fig. 6C), and the averaged $\Delta R_1\rho$ between 50 to 80 min post injection is 2.7 times larger for γB_1 = 300 Hz than for γB_1 = 3000 Hz. 2) Another difference is that the cortical $\Delta R_1\rho$ response reached a peak at ~15 min for the mannitol injection but increased slowly for the whole 80-min duration after the injection of 2DG. Assuming the contribution from the injection-induced osmolality increase to $\Delta R_1\rho$ is linearly dependent on injection dose, the contribution from the osmolality effect to the 2DG-CESL signal was estimated to be ¼ of the $\Delta R_1\rho$ of the mannitol data in Fig. 5B and plotted as the blue time course in Fig. 5C. At >40 min post-injection, the maximal contribution from the osmolality effect to the 2DG-CESL signal (blue line in Fig. 6C) is <20% of $\Delta R_1\rho$ at γB_1 = 300 Hz.

Discussions

Signal sources of 2DG-CESL: glucose metabolism weighting

The CESL approach is sensitive to both 2DG and 2DG6P. 2DG6P resides in the intracellular space while 2DG is located not only in the intracellular space but the intravascular and extravascular-extracellular spaces as well. It was reported that with a 0.5 g/kg 2DG injection, the brain concentration of 2DG6P was ~3 times less than 2DG at 5 minutes post-injection and rose to ~3 times higher than 2DG at 65 minutes post-injection (Kotyk et al., 1989). Thus, 2DG is dominant at early time points while 2DG6P is dominant at later time points. Our dose-dependent temporal characteristics can provide insights into the signal sources of glucoCESL. Right after intravenous injection of 2DG, CESL $R_1\rho$ increases slowly, indicating minimal contribution from intravascular 2DG which should reach a peak immediately after the injection (Jin et al., 2014). The magnitude of $R_1\rho$ changes within the initial ~20 minutes is nearly proportional to the dose of 2DG (Fig. 3). Previous studies showed the relationship between brain and plasma glucose level to be linear at a range of 4.5 mM to 30 mM plasma glucose (Choi et al., 2001). Injection of 1 g/kg of 2DG leads to a peak of ~250 to ~400 mg/dL (i.e., 14 to 22 mM) in the blood 2DG level (Jin et al., 2014; Nasrallah et al., 2013), thus 2DG transport across the BBB should not be rate-limiting. Consequently, the CESL signal is expected to be linearly correlated to the injected 2DG concentration and likely dominated by 2DG transport. At later time points (>30 min), the change in $R_1\rho$ is small and exhibits sublinear correlation to 2DG dose. Since phosphorylation of 2DG to 2DG6P is dependent on the availability of intracellular 2DG as well as CMRglu, the slowly produced 2DG6P does not accumulate linearly with injection dose. This metabolic process can explain sub-linear dependence of $\Delta R_1\rho$ on the injection dose at later time periods. Taken together, our 2DG-CESL intensity may be considered to be transport-weighted at the initial post-injection periods shifting to metabolism-weighting at later periods.

Because glucose metabolism and blood flow are tightly coupled under physiological conditions to meet metabolic requirements (Siesjo, 1978), one may postulate that the magnitude of 2DG-CESL response is strongly affected by CBF. To differentiate these two contributions to 2DG-CESL, isoflurane level was modulated. Since a higher isoflurane would suppress the uptake and metabolism of glucose but increase CBF (Lenz et al., 1999), the observation of smaller $\Delta R_1\rho$ with higher isoflurane level can be better explained by being dominated by lower metabolism rather than elevated CBF. Relative $\Delta R_1\rho$ value of 0.45, 0.33, and 0.19 s^{-1} for 0.5%, 1.5% and 2.2% isoflurane level is in good agreement with 2DG autoradiographic results, in which the CMRglu in the cortical area is about 45, 30 and 20 μmol·100g^{-1}·min^{-1} at similar isoflurane levels, respectively (Maekawa et al., 1986).

Our results also show that $\Delta R_1\rho$ is regionally heterogeneous with a higher change (~63–68%) in cortical gray matter than white matter and subcortical regions such as the globus pallidus. According to a previous 2DG autoradiographic study (Maekawa et al., 1986), the cerebral glucose metabolic rate in the cortex is ~66% and ~3 times higher than the globus pallidus and corpus callosum of rats under 0.5% isoflurane. The $\Delta R_1\rho$ contrast between cortex and globus pallidus agrees well with CMRglu data. The $\Delta R_1\rho$ contrast between the cortex and the corpus callosum is much lower than the CMRglu, which may be due to the partial-volume contribution of gray matter to the corpus callosum ROI with our limited spatial resolution.

Signal sources of 2DG-CESL: chemical exchange processes

Since the 2DG-CESL signal is indirectly measured from water, the relatively large dose may cause other physiological changes unrelated to glucose transport and metabolism such as osmolality effects and CBF increase (Horinaka et al., 1997). To distinguish chemical exchange vs. non-exchange contributions, two approaches were adopted. First, non-transportable mannitol was used assuming similar osmolality effects. In fact, 2DG-CESL is expected to have less osmolality contribution than the CESL signal of mannitol at the same dose, since osmolality gradients between blood and brain will be maintained for the non-transportable mannitol, but decrease over time for the transportable 2DG. The magnitude of glucoCESL signal induced by mannitol is not much smaller than that of 2DG at the initial period (e.g. <5 min) after injection but reduces to less than 20% of that by 2DG after 40 min post-injection. Another important difference is the dynamic properties of the two compounds. Dynamic $\Delta R_1\rho$ observed for mannitol injection is similar to a previous hemodynamic study showing that CBF response peaks at 15 minutes after the injection of 0.25 g/kg 2DG and returns nearly to baseline at 40 minutes (Medvedev et al., 1991). The much slower temporal characteristics for $\Delta R_1\rho$ response after 0.25 g/kg 2DG injection suggests that it is mainly due to transport and metabolism processes rather than vascular responses to injection. Clearly, the contribution from hemodynamic or osmolality effects to 2DG-CESL is minimal at >40 min post injection. Second, spin-lock power was modulated to separate exchangeable proton concentration changes (Δp term) and the γB_1-insensitive $\Delta R_{2,0}$ term in Eq. [3]. $\Delta R_1\rho$ has very different γB_1 dependence for mannitol and 2DG, confirming their different signal sources. Our data showed that the $\Delta R_1\rho$ response for 2DG should be mainly from the Δp term in Eq. [3], whereas the $\Delta R_1\rho$ response for mannitol would mainly be caused by the $\Delta R_{2,0}$ term.

Signal sources of 2DG-CESL: other possible sources

Large increase in $R_1\rho$ after both 2DG and mannitol injection was detected in the CSF region, which is independent of spin-lock power, indicating a non-chemical exchange contribution. In pixels containing both tissue and CSF, a change of their relative volume fractions can cause γB_1-insensitive $\Delta R_1\rho$. In our functional activation studies (Jin and Kim, 2010), an increase of blood volume leads to a reduction in the CSF volume fraction resulting in an increase of $R_1\rho$ which is independent of γB_1 (Jin and Kim, 2010; Jin and Kim, 2013). It has been reported that an injection of 0.2 g/kg 2DG almost doubles CBF (Horinaka et al., 1997), which can induce a significant increase in blood volume due to tight coupling between blood flow and volume. Thus, a decrease of CSF volume with smaller $R_1\rho$ value may explain the $R_1\rho$ increase after 2DG (and mannitol) injection in the CSF region.

Previous studies showed that 2DG6P reaches a peak at ~40 min after 0.5 g/kg of 2DG injection and then slowly decreases (Kotyk et al., 1989; Nasrallah et al., 2013). In contrast, the 2DG-CESL responses at >40 min after a 0.25 g/kg or 0.5 g/kg injection either sustain or slowly increase. The reason for these potential descrepancies is not clear, but one possibility is the detection of increased glucose signals in addition to 2DG and 2DG6P. Deuel et al. reported that 0.5 g/kg 2DG injection in awake rats induces blood glucose levels to increase from 4.4 mM to 16.6 mM at 2.5 hr later (Deuel et al., 1985). This slow elevation in blood glucose (hyperglycemia) would likely be transported to the brain tissue and may affect the 2DG-CESL response, especially after a long period (>1 hr).

In Paradigm 2, an isoflurane level of 0.5% was used while animals were paralyzed with pancuronium bromide. Several hormonal changes due to fear or anxiety at such low anesthesia levels (e.g., norepinephrine and epinephrine) may cause a change in the glucose metabolism rate as well as a breakdown of global glycogen stores and the release of glucose to the blood stream. Thus, the contribution from glucose due to hormonal changes cannot be excluded. However, since the quantitative $\Delta R_1\rho$ of 2DG-CESL is closely correlated with CMRglu, we expect that the observed higher 2DG-CESL response at 0.5 % isoflurane is mainly due to an increase of glucose metabolism associated with reduced anesthesia.

Comparison of glucoCEST and glucoCESL

Although both glucoCEST and glucoCESL techniques can detect 2DG and its metabolic product, their sensitivity and exact signal sources differ. CESL likely has higher sensitivity than CEST for the detection of 2DG (Jin et al., 2014; Zu et al., 2014) since CESL is less susceptible to small B_0 drift and has faster temporal resolution (Jin et al., 2014). Furthermore, it is known that the sensitivity of the CEST technique is optimal for slow chemical exchange applications (van Zijl and Yadav, 2011; Ward et al., 2000), i.e. where the chemical exchange rate between water and labile protons k is much smaller than their chemical shift δ, and spin-lock MRI is more suitable for studies of intermediate or fast chemical exchanges (Jin et al., 2011). The proton exchange between water and glucose and 2DG hydroxyl group was estimated to be around ~4600 s^{-1} under physiological conditions (Jin et al., 2014; Yadav et al., 2014), falling into the intermediate exchange regime at high magnetic fields (of 7 to 11 T) and into the fast exchange regime at clinical field strength (<3

T). Thus, the sensitivity advantage of glucoCESL would be expected to be even larger at lower clinical magnetic fields (Jin et al., 2014).

Temporal characteristics of CEST and CESL in the normal brain are quite different, especially during the plateau period of blood 2DG concentration after the injection of 0.5 to 1.0 g/kg 2DG. 2DG6P and blood 2DG maintain a relatively stable level during the 30–80 min post-injection period (Nasrallah et al., 2013). During the same period, glucoCEST signals return to the pre-injection baseline (Nasrallah et al., 2013) while glucoCESL signals sustain a relatively similar level (slightly increase or decrease) (Fig. 3A). This difference in CESL and CEST should be caused by the differential sensitivities of non-chemical exchange components and 2DG/2DG6P. First, the glucoCEST study with injection of L-glucose (which cannot be transported across the BBB, similar to mannitol used here) showed that glucoCEST is insensitive to the osmolality effect (Nasrallah et al., 2013). Since the contribution of osmolality effect is also small in glucoCESL (see Fig. 6), this cannot explain the temporal difference between CEST and CESL. Second, glucoCEST and glucoCESL have different sensitivities to different chemical exchange rates, as mentioned prior. Therefore, they may have different weightings between the extracellular and intracellular spaces, because chemical exchange rate is dependent on pH and the concentration of exchange catalysts, both of which may differ in these two pools. Third, blood flow and volume increase after 2DG injection may change susceptibility effects, which affect glucoCEST more than glucoCESL (Jin et al., 2014). To further understand the different signal sources of glucoCEST and glucoCESL, systematic comparison studies would be necessary in the future.

Technical issues of 2DG-CESL

The sensitivity of glucoCESL to 2DG is much higher than that of glucose, likely due to the fast metabolism of glucose as well as the accumulation of metabolized 2DG6P in cells. Consequently, the 2DG time course (Fig. 2D) is quite different from that of D-glucose where a peak was observed about 15–20 min after bolus injection (Jin et al., 2014) dropping to pre-injection baseline in ~60 minutes after the injected D-glucose was fully metabolized. However, the application of 2DG has a major limitation, namely its toxicity. While the usage of 2DG in humans is only limited to special cases with an oral dosage of less than 0.2 to 0.3 g/kg (Dwarakanath et al., 2009; Singh et al., 2005), recent studies show that a dose of 0.5 g/kg of FDG can be tolerated in anesthetized rats with minimal side effects to cerebral physiology and evoked BOLD-fMRI response to forepaw stimulation (Coman et al., 2014). In our studies, a dose of 0.25 g/kg 2DG was used to reduce its toxicity, while retaining sufficient sensitivity to enable glucose metabolism-related mapping.

CESL sensitivity is also dependent on spin-lock parameters. A higher spin-locking power will suppress the chemical exchange effect (Eq. [3]), and a lower spin-locking power may increase low-frequency fluctuations, such as those due to the BOLD effect (see the R_2-weighted response from Fig. 2B and 2C). While a spin-locking frequency of 500 Hz was adopted in this study (except Paradigm 4), the sensitivity of 2DG-CESL may slightly improve if this frequency is optimized. Additionally, CESL sensitivity may be further improved if better RF coil and/or advanced imaging techniques were adopted such as

parallel imaging. The threshold dose can be lower for conscious subjects where glucose utilization is higher than in the anesthetized condition (Lenz et al., 1999; Ori et al., 1986) and may also be reduced for pathological applications where glucose transport or metabolism is elevated compared to normal tissues such as in tumors.

Conclusion

The 2DG-CESL signal in the healthy rat brain is strongly dependent on the injection dose, anethesia level, brain regions, and the spin-lock power level. 2DG-CESL signals likely contain both transport and metabolisim components which are respectively more heavily weighted during the early and later response. With careful control of animal physiology, a single dose of 0.25 g/kg can provide sufficient sensitivity for high-resolution metabolic imaging under our settings. Our results suggest that 2DG-CESL may be a useful technique for the study of glucose transport and metabolism in normal and pathological brains.

Acknowledgments

We thank Kristy Hendrich for maintaining the 9.4 T system, and Julius Chung for proofreading. This work is supported by NIH grants EB003324, P30-NS076405 and P30-CA047904, and the Institute for Basic Science in Korea (IBS-R015-D1).

References

Chan KWY, McMahon MT, Kato Y, Liu GS, Bulte JWM, Bhujwalla ZM, Artemov D, van Zijl PCM. Natural D-glucose as a biodegradable MRI contrast agent for detecting cancer. Magnetic Resonance in Medicine. 2012; 68:1764–1773. [PubMed: 23074027]

Choi I-Y, Lee S-P, Kim S-G, Gruetter R. In vivo measurements of brain glucose transport using the reversible Michaelis-Menton model and simultaneous measurements of cerebral blood flow changes during hyperglycemia. Journal of Cerebral Blood Flow and Metabolism. 2001; 21:653–663. [PubMed: 11488534]

Cohen DM, Wei J, O'Brian Smith E, Gao X, Quast MJ, Sokoloff L. A method for measuring cerebral glucose metabolism in vivo by 13C-NMR spectroscopy. Magnetic Resonance in Medicine. 2002; 48:1063–1067. [PubMed: 12465118]

Coman D, Sanganahalli BG, Cheng D, McCarthy T, Rothman DL, Hyder F. Mapping phosphorylation rate of fluoro-deoxy-glucose in rat brain by F-19 chemical shift imaging. Magnetic Resonance Imaging. 2014; 32:305–313. [PubMed: 24581725]

de Leon MJ, Convit A, Wolf OT, Tarshish CY, DeSanti S, Rusinek H, Tsui W, Kandil E, Scherer AJ, Roche A, Imossi A, Thorn E, Bobinski M, Caraos C, Lesbre P, Schlyer D, Poirier J, Reisberg B, Fowler J. Prediction of cognitive decline in normal elderly subjects with 2-[(18)F]fluoro-2-deoxy-D-glucose/poitron-emission tomography (FDG/PET). Proceedings of the National Academy of Sciences of the United States of America. 2001; 98:10966–10971. [PubMed: 11526211]

Deuel RK, Yue GM, Sherman WR, Schickner DJ, Ackerman JJH. MONITORING THE TIME COURSE OF CEREBRAL DEOXYGLUCOSE METABOLISM BY P-31 NUCLEAR MAGNETIC-RESONANCE SPECTROSCOPY. Science. 1985; 228:1329–1331. [PubMed: 4001946]

Dwarakanath BS, Singh D, Banerji AK, Sarin R, Venkataramana NK, Jalali R, Vishwanath PN, Mohanti BK, Tripathi RP, Kalia VK, Jain V. Clinical studies for improving radiotherapy with 2-deoxy-D-glucose: present status and future prospects. Journal of Cancer Research and Therapeutics. 2009; 5(Suppl 1):S21–S26. [PubMed: 20009289]

Fox PT, Raichel ME. Stimulus rate dependence of regional cerebral blood flow in human striate cortex, demonstrated by positron emission tomography. Journal of Neurophysiology. 1984; 51:1109–1120. [PubMed: 6610024]

Garwood M, DelaBarre L. The return of the frequency sweep: Designing adiabatic pulses for contemporary NMR. Journal of Magnetic Resonance. 2001; 153:155–177. [PubMed: 11740891]

Grohn HI, Michaeli S, Garwood M, Kauppinen RA, Grohn OHJ. Quantitative T-1rho and adiabatic Carr-Purcell T-2 magnetic resonance imaging of human occipital lobe at 4 T. Magnetic Resonance in Medicine. 2005; 54:14–19. [PubMed: 15968651]

Heiss WD, Emunds HG, Herholz K. CEREBRAL GLUCOSE-METABOLISM AS A PREDICTOR OF REHABILITATION AFTER ISCHEMIC STROKE. Stroke. 1993; 24:1784–1788. [PubMed: 8248955]

Horinaka N, Artz N, Jehle J, Takahashi S, Kennedy C, Sokoloff L. Examination of potential mechanisms in the enhancement of cerebral blood flow by hypoglycemia and pharmacological doses of deoxyglucose. Journal of Cerebral Blood Flow and Metabolism. 1997; 17:54–63. [PubMed: 8978387]

Huang MT, Veech RL. Metabolic fluxes between [14C]2-deoxy-D-glucose and [14C]2-deoxy-D-glucose-6-phosphate in brain in vivo. Journal of Neurochemistry. 1985; 44:567–573. [PubMed: 3965622]

Ido T, Wan CN, Casella V, Fowler JS, Wolf AP, Reivich M, Kuhl DE. LABELED 2-DEOXY-D-GLUCOSE ANALOGS - F-18-LABELED 2-DEOXY-2-FLUORO-D-GLUCOSE, 2-DEOXY-2-FLUORO-D-MANNOSE AND C-14-2-DEOXY-2-FLUORO-D-GLUCOSE. Journal of Labelled Compounds & Radiopharmaceuticals. 1978; 14:175–183.

Jain VK, Kalia VK, Sharma R, Maharajan V, Menon M. Effects of 2-deoxy-D-glucose on glycolysis, proliferation kinetics and radiation response of human cancer cells. International Journal of Radiation Oncology, Biology, Physics. 1985; 11:943–950.

Jin T, Autio J, Obata T, Kim SG. Spin-locking versus chemical exchange saturation transfer MRI for investigating chemical exchange process between water and labile metabolite protons. Magnetic Resonance in Medicine. 2011; 65:1448–1460. [PubMed: 21500270]

Jin T, Kim S-G. Change of the cerebrospinal fluid volume during brain activation investigated by T1ρ-weighted fMRI. Neuroimag. 2010; 51:1378–1383.

Jin T, Kim SG. Characterization of non-hemodynamic functional signal measured by spin-lock fMRI. Neuroimage. 2013; 78:385–395. [PubMed: 23618601]

Jin T, Mehrens H, Hendrich K, Kim SG. Mapping brain glucose uptake with chemical exchange-sensitive spin-lock magnetic resonance imaging. Journal of Cerebral Blood Flow and Metabolism. 2014; 34:1402–1410. [PubMed: 24865996]

Kotyk JJ, Rust RS, Ackerman JJH, Deuel RK. Simultaneous in vivo monitoring of cerebral deoxyglucose and deoxyglucose-6-phosphate by 13C{1H} nuclear magnetic resonance spectroscopy. Journal of Neurochemistry. 1989; 53:1620–1628. [PubMed: 2795021]

Lenz C, Frietsch T, Futterer C, Rebel A, van Ackern K, Kuschinsky W, Waschke KF. Local coupling of cerebral blood flow to cerebral glucose metabolism during inhalational anesthesia in rats: desflurane versus isoflurane. Anesthesiology. 1999; 91:1720–1723. [PubMed: 10598615]

Ma Y, Eidelberg D. Functional imaging of cerebral blood flow and glucose metabolism in Parkinson's disease and Huntington's disease. Molecular Imaging and Biology. 2007; 9:223–233. [PubMed: 17334854]

Maekawa T, Tommasino C, Shapiro HM, Keifer-Goodman J, Kohlenberger RW. Local cerebral blood flow and glucose utilization during isoflurane anesthesia in the rat. Anesthesiology. 1986; 65:144–151. [PubMed: 3740503]

Matz K, Keresztes K, Tatschl C, Nowotny M, Dachenhausenm A, Brainin M, Tuomilehto J. Disorders of glucose metabolism in acute stroke patients - An underrecognized problem. Diabetes Care. 2006; 29:792–797. [PubMed: 16567817]

Medvedev OS, Oranovskaya EV, Ashirova OP, Murashev AN. REACTIONS OF THE SYSTEMIC AND REGIONAL HEMODYNAMICS TO METABOLIC STRESS INDUCED BY 2-DEOXYGLUCOSE. Bulletin of Experimental Biology and Medicine. 1991; 111:132–135.

Moses WW. Fundamental Limits of Spatial Resolution in PET. Nuclear Instruments & Methods in Physics Research. Section A: Accelerators, Spectrometers, Detectors and Associated Equipment. 2011; 648(Supplement 1):S236–S240.

Nasrallah FA, Pages G, Kuchel PW, Golay X, Chuang KH. Imaging brain deoxyglucose uptake and metabolism by glucoCEST MRI. Journal of Cerebral Blood Flow and Metabolism. 2013; 33:1270–1278. [PubMed: 23673434]

Ori C, Dam M, Pizzolato G, Battistin L, Giron G. EFFECTS OF ISOFLURANE ANESTHESIA ON LOCAL CEREBRAL GLUCOSE-UTILIZATION IN THE RAT. Anesthesiology. 1986; 65:152–156. [PubMed: 3740504]

Rivlin M, Horev J, Tsarfaty I, Navon G. Molecular imaging of tumors and metastases using chemical exchange saturation transfer (CEST) MRI. Scientific Reports. 2013; 3:3045. [PubMed: 24157711]

Siesjo, B. Brain Energy Metabolism. New York: Wiley; 1978.

Silverman DHS, Small GW, Chang CY, Lu CS, de Aburto MAK, Chen W, Czernin J, Rapoport SI, Pietrini P, Alexander GE, Schapiro MB, Jagust WJ, Hoffman JM, Welsh-Bohmer KA, Alavi A, Clark CM, Salmon E, de Leon MJ, Mielke R, Cummings JL, Kowell AP, Gambhir SS, Hoh CK, Phelps ME. Positron emission tomography in evaluation of dementia - Regional brain metabolism and long-term outcome. Jama-Journal of the American Medical Association. 2001; 286:2120–2127.

Singh D, Banerji AK, Dwarakanath BS, Tripathi RP, Gupta JP, Mathew TL, Ravindranath T, Jain V. Optimizing cancer radiotherapy with 2-deoxy-d-glucose dose escalation studies in patients with glioblastoma multiforme. Strahlentherapie und Onkologie. 2005; 181:507–514. [PubMed: 16044218]

Sokoloff L, Reivich M, Kennedy C, Des Rosiers MH, Patlak CS, Pettigrew KD, Sakurada O, Shinohara M. The [14C]deoxyglucose method for the measurement of local cerebral glucose utilization: theory, procedure, and normal values in the conscious and anesthetized albino rat. Journal of Neurochemistry. 1977; 28:897–916. [PubMed: 864466]

Strupp JP. Stimulate: A GUI based fMRI analysis software package. Neuroimage. 1996; 3:S607.

Thenuwara K, Todd M, Brian JEJ. Effect of Mannitol and Furosemide on Plasma Osmolality and Brain Water. Anesthesiology. 2002; 96:416–421. [PubMed: 11818776]

Trott O, Palmer AG. R-1rho relaxation outside of the fast-exchange limit. Journal of Magnetic Resonance. 2002; 154:157–160. [PubMed: 11820837]

van Zijl PCM, Yadav NN. Chemical Exchange Saturation Transfer (CEST): what is in a name and what isn't? Mag Reson Med. 2011; 65:927–948.

Walker-Samuel S, Ramasawmy R, Torrealdea F, Rega M, Rajkumar V, Johnson SP, Richardson S, Goncalves M, Parkes H, Arstad E, Thomas D, Pedley R, Lythgoe M, Golay X. In vivo imaging of glucose uptake and metabolism in tumors. Nature Medicine. 2013; 19:1067–1072.

Ward KM, Aletras AH, Balaban RS. A new class of contrast agents for MRI based on proton chemical exchange dependent saturation transfer (CEST). Journal of Magnetic Resonance. 2000; 143:79–87. [PubMed: 10698648]

Yadav NN, Xu J, Bar-Shir A, Qin Q, Chan KW, Grgac K, Li W, McMahon MT, van Zijl PC. Natural D-glucose as a biodegradable MRI relaxation agent. Magnetic Resonance in Medicine. 2014; 72:823–828. [PubMed: 24975029]

Yong SW, Yoon JK, An YS, Lee PH. A comparison of cerebral glucose metabolism in Parkinson's disease, Parkinson's disease dementia and dementia with Lewy bodies. European Journal of Neurology. 2007; 14:1357–1362. [PubMed: 17941855]

Zu Z, Spear J, Li H, Xu J, Gore JC. Measurement of regional cerebral glucose uptake by magnetic resonance spin-lock imaging. Magnetic Resonance Imaging. 2014; 32:1078–1084. [PubMed: 24960367]

Highlights

- Chemical exchange-sensitive spin-lock (CESL) MRI signal increases linearly with 2DG dose at initially but not at later periods.
- The 2DG-CESL signal is reduced at higher isoflurane anesthesia levels correlating well with glucose metabolism rate.
- 2DG-CESL signal shows spatial heterogeneity and is higher in gray matter than white matter.
- 2DG-CESL predominantly measures chemical exchange-related signals in the extravascular space.

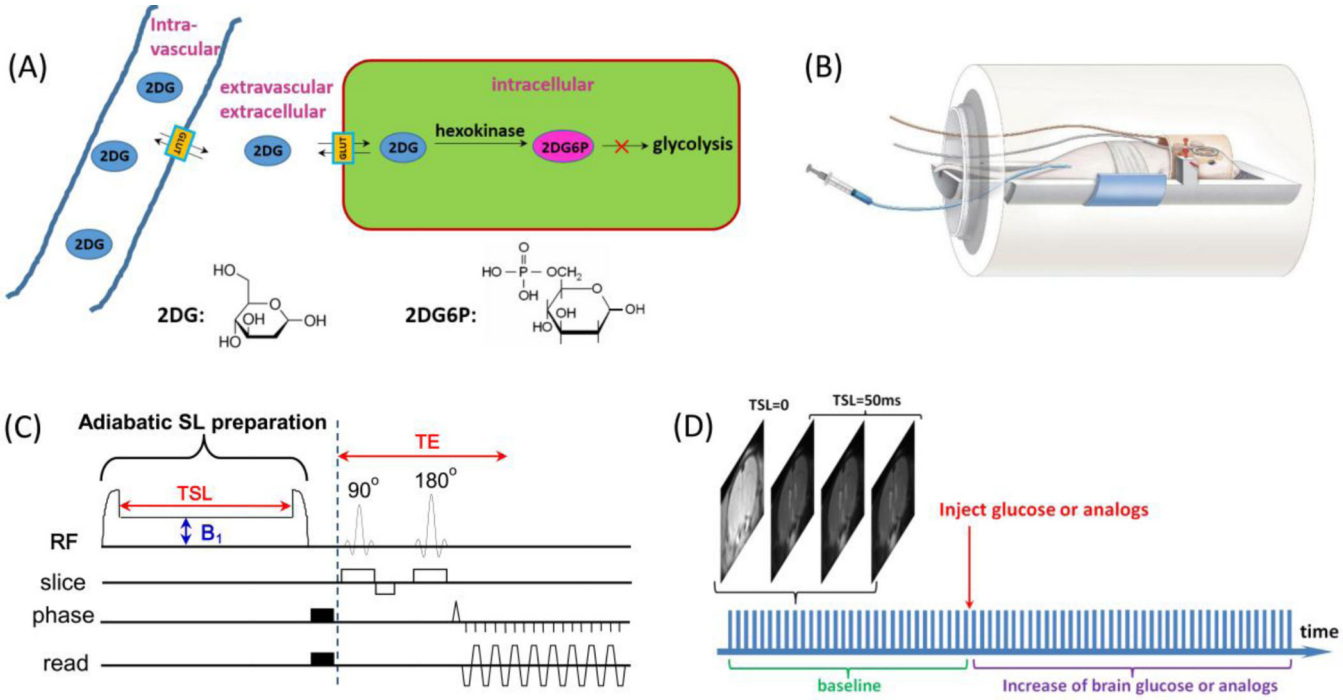

Fig. 1. Experimental setup and protocol for 2DG-CESL study

(A) A schematic illustration of the transport and metabolism of 2DG in brain. The injected 2DG in the intravascular space is transported by glucose transporters across the blood brain barrier to the extravascular-extracellular space and followed by uptake into the intracellular space where it is phosphorylated into 2DG6P. Both 2DG and 2DG6P have hydroxyl groups which rapidly exchange with water protons and can be detected by the CESL technique. (B) A schematic illustration of our animal-experiment setup shows a combination of volume coil transmit and surface coil receive, and the 2DG is injected through a venous line. (C) The pulse sequence for chemical exchange-sensitive spin-lock (CESL) MRI used in this study contains an adiabatic spin-lock (SL) preparation followed by spin-echo echo planar imaging for imaging acquisition. B_1: spin-lock power level, TSL: spin-lock time, TE: echo time. (D) Each glucoCESL MRI experiment was performed by repeated acquisitions of four images (one TSL = 0 ms and three TSL = 50 ms) before and after injection of 2DG or mannitol. A time series of $R_1\rho$ (=1/$T_1\rho$) was generated from data with two TSL values.

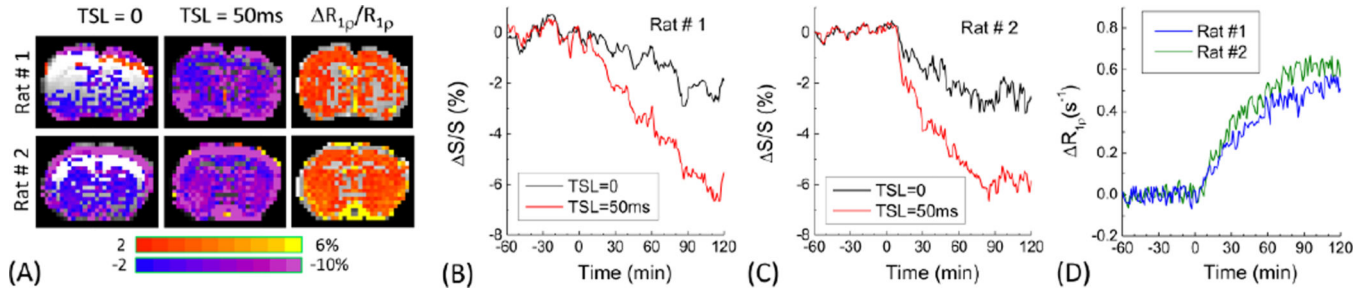

Fig. 2. Spin-echo vs. spin-lock MRI results

Comparison of the percent change maps (A), time courses of T_2-weighted (TSL = 0 and TE = 30 ms) and $T_1\rho$-weighted (TSL = 50 ms and TE = 30 ms) signals (B and C), and calculated $R_1\rho$ responses (D) from two representative animals. 0.5 g/kg of 2DG was intravenously injected to 1.5% isoflurane anesthetized rats at time 0. Data in (B–D) was obtained from all pixels of brain in all slices. Large fluctuations were observed in B and C, but not in D where the T_2 contribution during TE was removed.

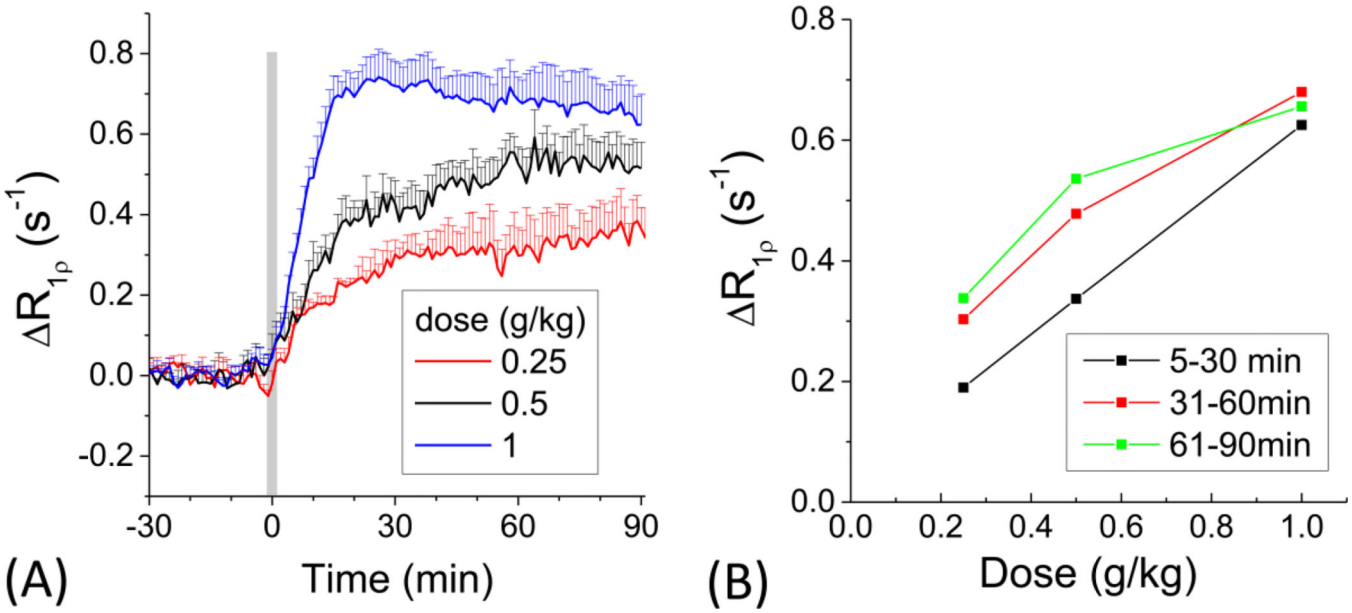

Fig. 3. 2DG dose dependency

Time courses of the CESL $R_1\rho$ change (A) obtained from the rat cortex for three 2DG doses of 0.25 (n=4 animals), 0.5 (n=6) and 1 g/kg (n=7). Animals were maintained under 1.5% isoflurane. (B) Dose-dependent $R_1\rho$ changes in 5 to 30 min, 31 to 60 min, and 61 to 90 min periods. The $R_1\rho$ change is linearly dependent on the injection dose at an early time, but not later time. This suggests that the early response is sensitive to 2DG transport while the later time is more weighted to metabolized 2DG6P. Error bars: SD.

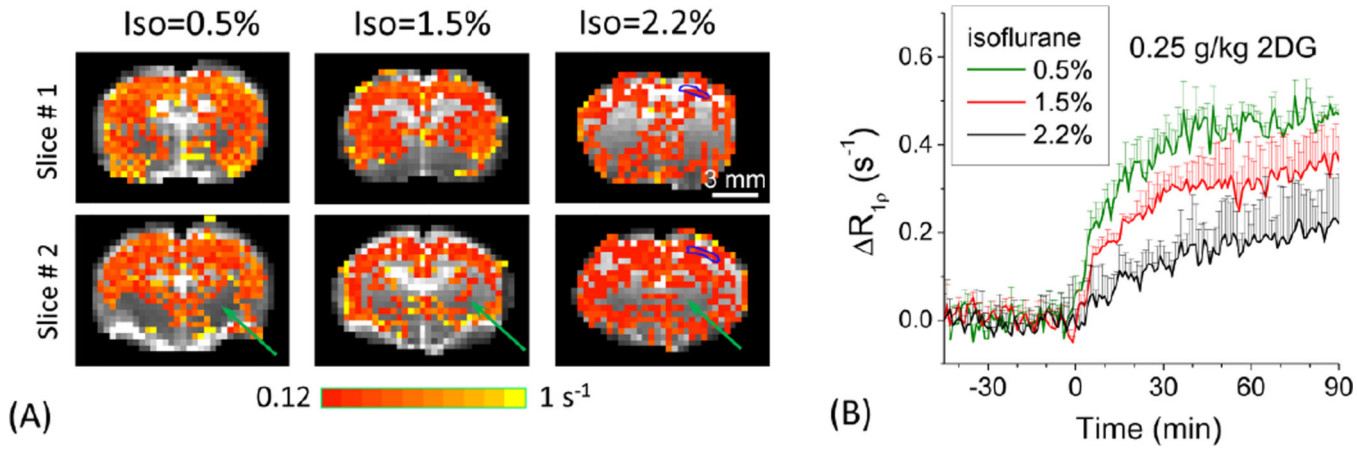

Fig. 4. Anesthesia level dependency

Percent change maps of 2DG-CESL $R_1\rho$ in representative animals (A) and averaged time courses from cortical ROIs under 0.5% (n=6 animals), 1.5% (n=5), and 2.2% (n=4) isoflurane. A 0.25 g/kg of 2DG dose was used. The blue contoured ROI was shown in 2.2% isoflurane data in the right hemisphere (A) and used for obtaining time courses (B). 2DG-CESL correlates well with glucose metabolism. Data were shown as mean ± SD.

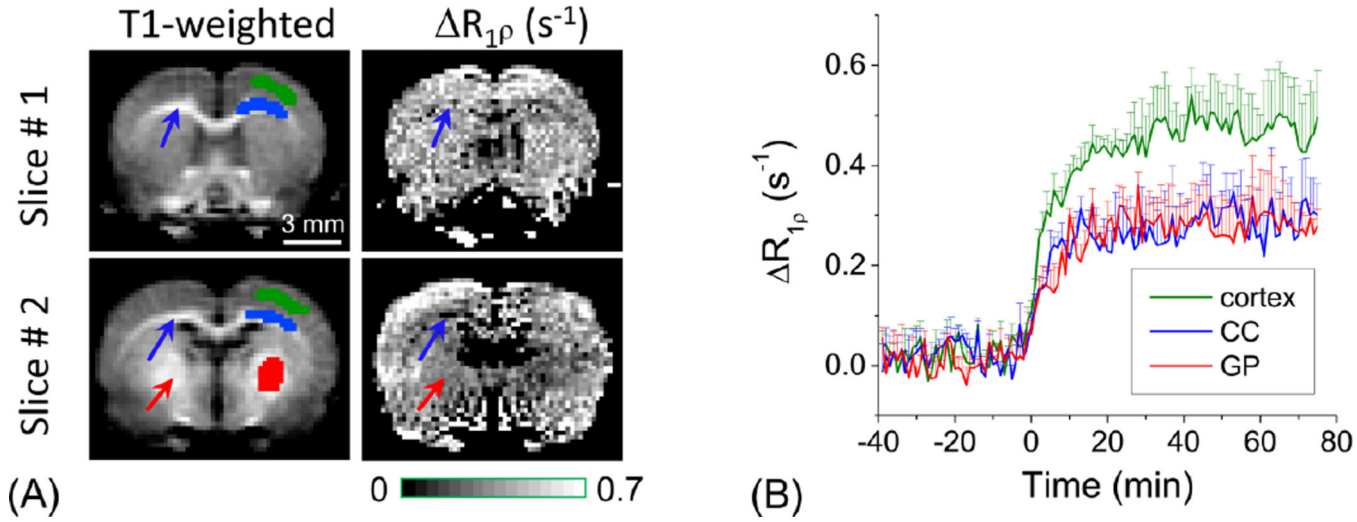

Fig. 5. Regional heterogeneity measured by high-resolution 2DG-CESL

Comparison of T_1-weighted images and maps of $R_1\rho$ changes (two slices) (A), and the time courses from the cortex, corpus callosum (CC, blue arrows), and globus pallidus (GP, red arrows) ROI (B). $R_1\rho$ changes with 333×333×1500 μm^3 resolution were measured with 0.25 g/kg 2DG injection under 0.5% isoflurane. Pixels of ROIs were shown as green, blue and red color in the right hemisphere for the cortex, CC, and GP, respectively. Lower $R_1\rho$ change was observed in the CC and the globus pallidus indicating that 2DG-CESL correlates with glucose metabolism. Error bars: SD

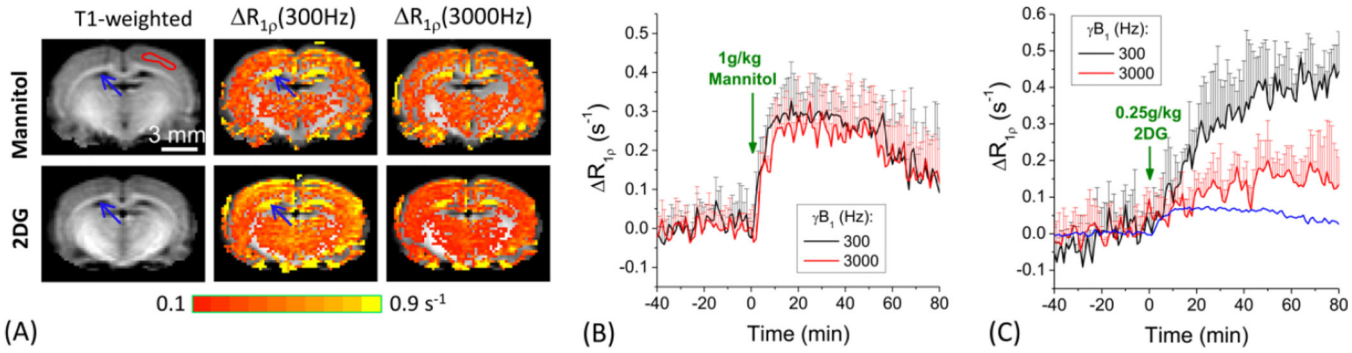

Fig. 6. Signal sources of 2DG-CESL

$R_1\rho$ changes were measured at two spin-lock power levels with 1 g/kg of mannitol (n=4 animals) vs. 0.25 g/kg 2DG injection (n=4). Rats were anesthetized with 0.5% isoflurane. $R_1\rho$ change maps were overlaid on T_1-weighted images (A); and the time courses were obtained from cortical ROIs (shown in one hemisphere by the red contour in T_1-weighted image) for mannitol (B) and 2DG (C). Data were shown as mean ± SD. Assuming the contribution from the injection-induced osmolality increase to $\Delta R_1\rho$ is linearly dependent on the injection dose, the contribution from the osmolality effect to the 2DG-CESL signal were estimated. The blue time course in (C) represents the non-chemical exchange contribution to the CESL signal, taken as ¼ of the $\Delta R_1\rho$ time course of mannitol injection. Large $R_1\rho$ change at the ventricle area (blue arrows) is due to a relative volume change of CSF in the voxel (see text).